

Flexible organic solar cells composed of P3HT:PCBM using chemically doped graphene electrodes

Sangchul Lee¹, Jun-Seok Yeo², Yongsung Ji², Chunhum Cho²,
Dong-Yu Kim^{1,2}, Seok-In Na³, Byoung Hun Lee^{1,2} and Takhee Lee⁴

¹ Department of Nanobio Materials and Electronics, Gwangju Institute of Science and Technology, Gwangju 500-712, Korea

² School of Materials Science and Engineering, Gwangju Institute of Science and Technology, Gwangju 500-712, Korea

³ Graduate School of Flexible and Printable Electronics, Chonbuk National University, Jeonju-si, Jeollabuk-do, 561-756, Korea

⁴ Department of Physics and Astronomy, Seoul National University, Seoul 151-747, Korea

E-mail: nsi12@jbnu.ac.kr and tlee@gist.ac.kr

Received 10 February 2012, in final form 4 May 2012

Published 10 August 2012

Online at stacks.iop.org/Nano/23/344013

Abstract

Flexible organic solar cells (OSCs) composed of blended films of poly(3-hexylthiophene) (P3HT) and [6,6]-phenyl-C61-butyric acid methyl ester (PCBM) were fabricated and investigated with chemically doped multilayer graphene films as transparent and conducting electrodes on plastic substrates. The sheet resistance of the chemically doped graphene film was reduced to half of its original value, resulting in a significant performance enhancement of OSCs featuring doped graphene electrodes. Moreover, there was no substantial variation observed in the fill factor and power conversion efficiency values of the flexible OSCs under bending conditions. A power conversion efficiency of ~2.5% for flexible OSCs with doped graphene electrodes was observed under bending conditions, even up to a 5.2 mm bending radius.

(Some figures may appear in colour only in the online journal)

1. Introduction

One-dimensional bulk heterojunction organic solar cells (OSCs) have attracted considerable interest due to their potential for low-cost and large-area processes and their light weight, solution processability, and flexibility [1–3]. OSCs are of interest in producing portable, transparent, and flexible devices because such properties will be important in future flexible-device applications [4]. Indium tin oxide (ITO) has been the dominant material used as a transparent electrode. However, the price of ITO is continuously increasing due to the limited supply of indium and its high demand in industrial products [5]. Furthermore, ITO has an inherent mechanical brittleness that makes it unsuitable for flexible devices [4]. To overcome such drawbacks, alternative electrodes, such

as conducting polymers, carbon nanotubes, and indium-free oxide electrodes, are being investigated [6–10].

Among the various transparent-electrode materials that are available, graphene, a two-dimensional conducting sheet, has been proposed as a promising ITO alternative due to its remarkable optical, mechanical, and electrical properties [11]. For example, graphene films synthesized by chemical vapor deposition (CVD) have been used as transparent electrodes for electronic and optical devices, such as memories [12], touch-pad panels [13], light-emitting diodes [14], and liquid-crystal display devices [15]. Graphene films are also being applied to OSCs as transparent and conducting electrodes. In OSCs, the power conversion efficiency (PCE) is the major factor in evaluating the performance of devices. Until now, the PCE values of graphene-electrode OSCs have been reported to be

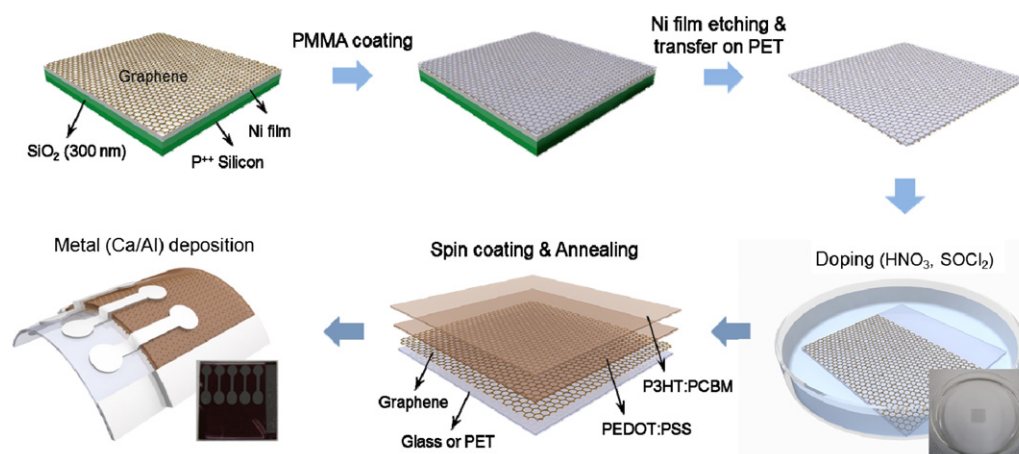


Figure 1. Schematics of the processes used to fabricate flexible OSCs. The inset images show an MLG film (lower right) and fabricated devices (lower left).

in the range of 0.08–2.60% [16–18], which is lower than the PCE values of state-of-the-art OSCs made with conventional ITO electrodes of approximately 8.5% [19, 20]. Thus, the PCE of graphene-electrode OSCs must be improved to make graphene a potential replacement for ITO.

In addition, bendable OSC devices have recently gained attention for flexible-device applications. Because organic materials are inherently flexible, flexible OSCs require a soft substrate and soft electrode layers in their device structures. In the flexible OSCs reported to date, ITO is still the most widely used electrode material, but its PCE values of 2.2–3.7% are poorer than those of inflexible ITO electrode OSCs. Additionally, ITO has limitations as a flexible electrode due to its mechanically inferior properties. Hence, it is worth investigating graphene for use in conducting and transparent electrodes in flexible OSCs and ultimately improving the PCEs of such devices. The PCE can be enhanced in several ways, such as improving the quality of the graphene films, the method through which these films are transferred, the device structure, and the fabrication process. Of these, lowering the sheet resistance of graphene is a particularly efficient strategy.

Hong *et al* demonstrated CVD-grown multilayer graphene electrodes with a sheet resistance (R_s) of $\sim 30 \Omega/\square$, which is considered one of the lowest R_s values reported to date [13]. However, most graphene films reported in the literature have shown a high R_s of a few hundred Ω/\square or more [21]. To lower the R_s , Kong *et al* recently suggested chemical doping. The resultant multilayer graphene film in their OSCs showed an R_s of 300–500 Ω/\square [22]. This finding indicated that the development of chemically doped graphene electrodes for flexible OSCs is important for achieving efficient flexible solar cells.

Here, we report the development of high performance, flexible OSCs with doped graphene electrodes. The CVD-grown multilayer graphene (MLG) films (thickness $< \sim 15$ nm) were chemically doped and used as conductive, transparent, and flexible electrodes. After conducting experiments with different dopants, we obtained sheet resistance values for the MLG films that were twofold less than the sheet resistance of a pristine (undoped) MLG film. Using the doped

MLG electrodes, we fabricated flexible OSCs with PCEs that reached 2.6%, which is considered a high value among the values reported for graphene-electrode-based OSCs. The performance of devices fabricated with our doped graphene electrodes remained nearly unchanged under various bending conditions, demonstrating that doped graphene may be a good candidate as a transparent-electrode material for high performance, flexible solar cells in terms of the enhanced PCE values.

2. Experimental details

The process followed to fabricate OSCs with doped graphene electrodes is illustrated in figure 1. We synthesized the MLG film by a chemical vapor deposition method. To synthesize the MLG, first, 300 nm-thick Ni-coated substrates were loaded and pre-annealed at 300 °C under a 200 sccm flow of Ar mixed with 4% H₂ for 30 min. Then, the temperature was increased to 900 °C. Subsequently, the MLG film was grown at 900 °C under a 5 sccm flow of methane and a 150 sccm flow of 4% H₂ in an Ar mixture for 5 min. After the growth, the MLG film was rapidly cooled down [23].

The grown MLG film was rinsed with deionized water more than three times; then it was transferred from deionized water onto a glass or poly(ethylene terephthalate) (PET) substrate using a scooping technique and subsequently doped with nitric acid (HNO₃, purchased from OCI Company, Ltd) or thionyl chloride (SOCl₂, purchased from Fluka) by dipping for 2 h. The doped MLG film was dried by blowing with N₂ gas. To prepare the OSC device, poly(3, 4-ethylenedioxythiophene):poly(styrenesulfonate) (known as PEDOT:PSS, Baytron P VPAI 4083, purchased from H. C. Starck) was spun on at 5000 rpm for 40 s as a buffer layer, followed by annealing at 110 °C for 10 min, which produced a film that was approximately 30 nm thick. A bulk heterojunction blend film of poly(3-hexylthiophene) (P3HT) and 1-(3-methoxycarbonyl)-propyl-1-phenyl-(6, 6)C₆₁ (PCBM) (P3HT:PCBM = 1:1) was used. For the deposition of photoactive layers, 25 mg of P3HT

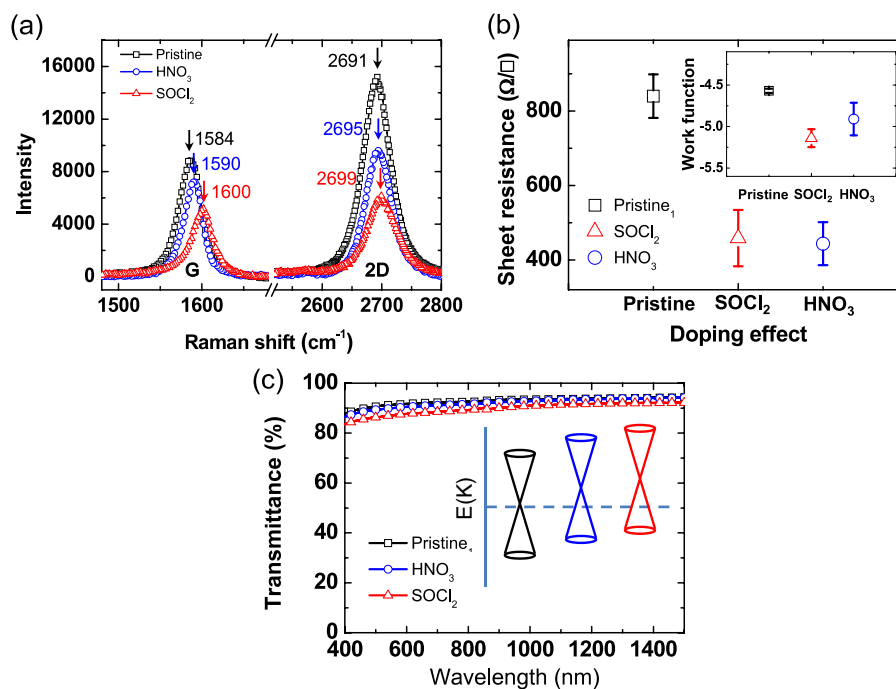


Figure 2. (a) Raman spectra of pristine graphene (open black squares), HNO_3 -doped graphene (open blue circles), and SOCl_2 -doped graphene (open red triangles). (b) Sheet resistance of pristine and doped graphene films. The inset shows the work functions of pristine and doped graphene films. (c) Transmittance characteristics of pristine (undoped) and HNO_3 - or SOCl_2 -doped MLG films. The inset shows a schematic of the change in the work function of the doped MLG films.

(purchased from Rieke Metals) and 25 mg of PCBM (purchased from Nano-C) were dissolved in 1 ml of 1, 2-dichlorobenzene. The P3HT and PCBM blend was stirred at 50°C for ~ 12 h in a N_2 -filled glove box to obtain a homogeneous mixture. Then, the solution was spin coated at 700 rpm for 60 s onto glass or PET substrates, followed by solvent annealing inside a covered glass jar for 2 h and thermal annealing at 110°C for 10 min, which produced an ~ 220 nm-thick active layer. Finally, Ca/Al (20 nm/100 nm) layers were deposited as the OSC cathode using a thermal evaporator at a pressure of 10^{-6} Torr.

3. Results and discussion

3.1. The doping effect on graphene films

Figure 2 shows the doping effect on the MLG film. Chemical dopants were chosen because doping is an easy approach to tailor the electronic properties of graphene films [20]. The p-doping materials HNO_3 and SOCl_2 were used; the transmittance of the doped MLG films remained nearly unchanged. We investigated the Raman spectra of the MLG films on Si/SiO₂ substrates before and after doping, as shown in figure 2(a). The Raman spectra were obtained with a laser excitation energy of 514 nm. After doping for 2 h, the G peak shifted to longer wavelengths for both dopants, which confirmed that the MLG was effectively p-doped in both cases [19]. The G band was located at 1584 cm^{-1} for pristine (undoped) graphene and at 1590 cm^{-1} and 1600 cm^{-1} for the HNO_3 -doped and SOCl_2 -doped MLG films, respectively.

Although other factors such as temperature, surface charge, and strain can shift the G band [24], such effects can be excluded here because all of the devices were fabricated and measured under identical experimental conditions. The 2D peak is also influenced by doping because its position reflects the increased electron concentration in the system [25]. As shown in figure 2(a), the 2D peak shifted under both doping conditions. Additionally, the intensity ratio of the G and 2D peaks ($I(2D)/I(G)$) can also explain the doping effect. The doped MLG films exhibited an increase in the $I(2D)/I(G)$ intensity from 0.55 for the pristine MLG film to 0.75 and 0.83 for the HNO_3 -doped and SOCl_2 -doped MLG films, respectively. These observations also confirm that the HNO_3 - or SOCl_2 -treated MLG films were effectively doped.

3.2. The performance of organic solar cells with doped graphene electrodes

After doping, the conductivity of the MLG films was significantly improved, as shown in figure 2(b). The sheet resistance of the pristine MLG film was $\sim 850\ \Omega/\square$; for the HNO_3 - and SOCl_2 -doped MLG films it was reduced by approximately one half to $\sim 450\ \Omega/\square$, while the transmittance of the doped MLG films remained nearly unchanged in the visible region (over 90% on average from 400 to 1400 nm), as shown in figure 2(c). In addition, we found that the work function of the MLG films changed after doping, as shown in the inset of figure 2(b). The work functions (measured with a Kelvin probe) of the HNO_3 -doped and SOCl_2 -doped MLG films changed to 4.9 eV and 5.1 eV, respectively, compared with 4.6 eV for the pristine MLG film.

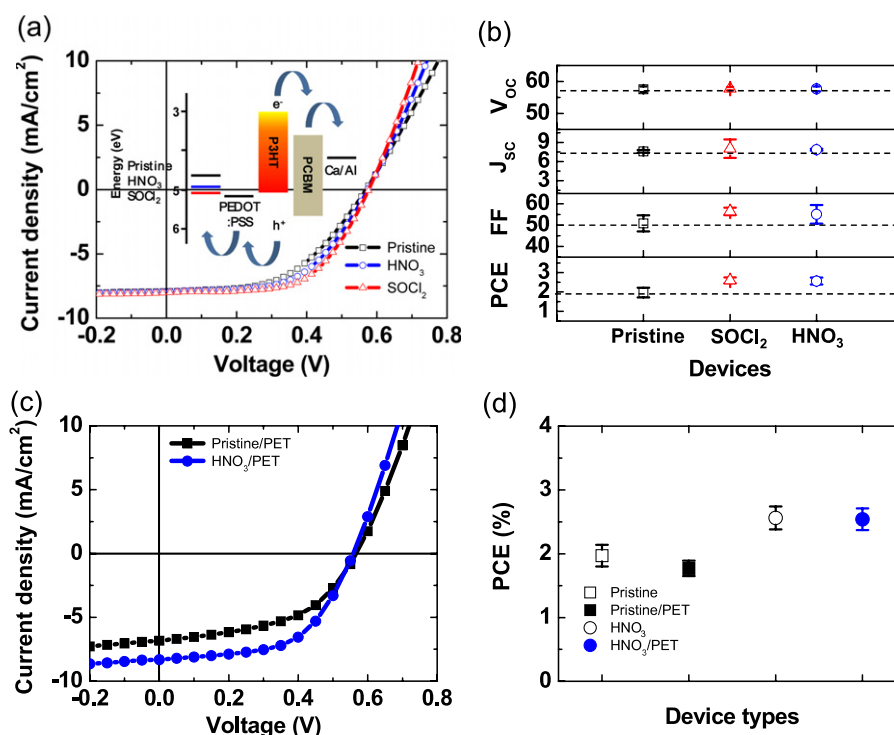


Figure 3. (a) Current–voltage characteristics of OSCs with pristine and HNO₃- or SOCl₂-doped MLG electrodes. The inset is the energy band diagram. (b) V_{OC} , J_{SC} , FF, and PCE values of OSCs with pristine and HNO₃- or SOCl₂-doped MLG electrodes. (c) Current–voltage characteristics of flexible OSCs with pristine and HNO₃-doped MLG electrodes. (d) Comparisons of the PCE values of flat (pristine and HNO₃) and flexible (pristine/PET and HNO₃/PET) OSCs with those of pristine and HNO₃-doped MLG electrodes.

We examined the performance of OSCs composed of P3HT:PCBM polymer. Pristine and MLG films with different dopants were first prepared as transparent and conducting electrodes on a (nonflexible) glass substrate. The current density–voltage (J – V) characteristics of the OSC devices with pristine (black open squares), HNO₃-doped (blue open circles), and SOCl₂-doped MLG electrodes (red open triangles) are shown in figure 3(a). The energy-level alignments measured by the Kelvin probe are shown in the inset of figure 3(a). The photovoltaic characteristics of the fabricated OSCs were characterized under a simulated A.M. 1.5 G light source with 100 mW cm^{−2} of illumination at room temperature. The performance parameters are summarized in figure 3(b) and table 1. The performances of the OSCs with pristine MLG electrodes were relatively inferior: a short-circuit current density (J_{SC}) of 7.5 mA cm^{−2}, an open-circuit voltage (V_{OC}) of 0.58 V, a fill factor (FF) of 52.5%, and a PCE of 1.97 ± 0.25%. In contrast, the OSCs with HNO₃- and SOCl₂-doped MLG electrodes exhibited better cell performance: J_{SC} of 7.9 and 8.0 mA cm^{−2}, V_{OC} of 0.58 and 0.58 V, FF of 55.2 and 59.1%, and PCE of 2.56 ± 0.18 and 2.60 ± 0.15%, respectively.

By comparing the doped and undoped graphene electrodes, the enhanced PCE of the OSCs with doped graphene electrodes was determined to be mainly due to improvements in the FF and J_{SC} rather than the V_{OC} , as shown in figure 3(b) and table 1. Although the work function of the doped graphene electrodes was higher than that of the pristine graphene electrode (inset of figure 2(b)), the V_{OC}

Table 1. Summary of the photovoltaic parameters of organic solar cells with conventional graphene and doped graphene electrodes.

Substrate	Electrode (anode)	V_{OC} (V)	J_{SC} (mA cm ^{−2})	FF (%)	PCE (%)
PET	GR	0.56	7.5	42.4	1.77 ± 0.12
	HNO ₃ -GR	0.56	8.3	55.9	2.54 ± 0.17
glass	GR	0.58	7.5	52.5	1.97 ± 0.25
	HNO ₃ -GR	0.58	7.9	55.2	2.56 ± 0.18
	SOCl ₂ -GR	0.58	8	59.1	2.60 ± 0.15

value was similar in all cases because the V_{OC} is mainly determined by the difference between the highest occupied molecular orbital (HOMO) level of the donor (P3HT) and the lowest unoccupied molecular orbital (LUMO) of the acceptor (PCBM) when there is an Ohmic contact between the electrodes and the active layer [26]. The OSCs with the doped graphene electrodes exhibited better FF and J_{SC} values than those with pristine graphene electrodes. Considering the fact that all of the materials and processes used to fabricate the OSCs were identical, except for the doped or undoped MLG electrodes, and that the FF and J_{SC} values of the OSCs are critically dependent on the sheet resistances of the transparent electrodes [8], the higher FF and J_{SC} values in the OSCs with doped graphene are attributed to the lower sheet resistances of the doped films (figure 2(b)) [20], which is confirmed by the J – V curves in figure 3(a).

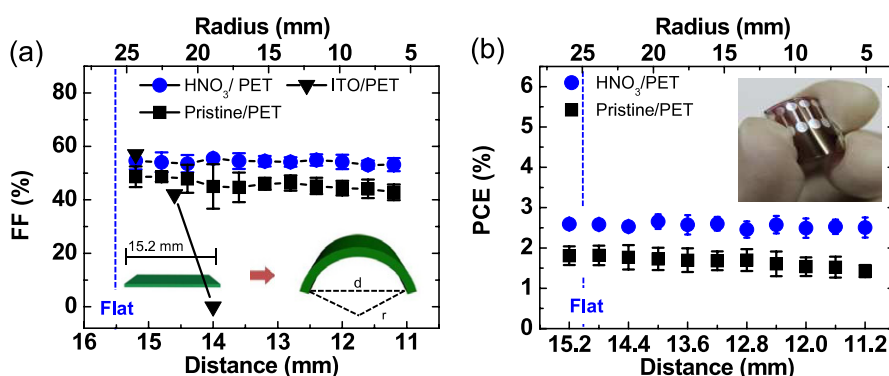


Figure 4. (a) FF and (b) PCE values of flexible OSCs with pristine and HNO₃-doped MLG electrodes under different bending conditions. The insets in ((a), (b)) show the bending conditions, and the inset in (b) shows a photograph of bent OSC devices.

3.3. The performance of flexible organic solar cells with doped graphene electrodes

It is also important to incorporate higher performance doped MLG electrodes into flexible OSC devices to determine whether device performance is maintained under bending. We fabricated flexible OSCs under identical fabrication conditions on plastic PET substrates. Figure 3(c) shows the J - V characteristics of OSCs with pristine and HNO₃-doped MLG electrodes on PET substrates. Note that flexible OSCs with SOCl₂-doped MLG electrodes could not be fabricated because SOCl₂ is acidic enough to melt the PET substrate. The OSCs with pristine MLG electrodes on PET substrates had a V_{OC} of 0.56 V, a J_{SC} of 7.5 mA cm⁻², an FF of 42.4%, and a PCE of 1.77 ± 0.12%. In contrast, the OSCs with HNO₃-doped MLG electrodes had a V_{OC} of 0.56 V, a J_{SC} of 8.3 mA cm⁻², an FF of 55.9%, and a PCE of 2.54 ± 0.17%. The higher PCE for OSCs on PET substrates with doped MLG electrodes resembled the trend for nonflexible OSCs on glass substrates (figures 3(a) and (b)), which indicates that the doped graphene-electrode OSCs operated well on flexible PET substrates.

Flexible OSCs with doped and undoped MLG electrodes were studied by monitoring the device performance during a bending test. We investigated the performance stability of the flexible OSCs under different bending conditions. The degree of bending was expressed by the radius of curvature (r) or distance (d), which was measured between two end points of the arc, as shown in the insets in figures 4(a) and (b). Figure 4(a) shows the FF under the bending condition. Although the bending was increased (i.e., the distance was shortened from 15.2 to 11.2 mm; the radius was changed from 27 to 5.2 mm), the FF values of OSCs with HNO₃-doped and undoped MLG electrodes remained almost unchanged. Considering the fact that the FF and J_{SC} values depend heavily on the R_s of the electrodes [27], such negligible variation in their values indicates that the MLG electrode is flexible and does not suffer from severe cracks or defect formation in the graphene films under the given bending conditions.

We also investigated the PCEs of OSCs with HNO₃-doped and undoped MLG electrodes under bending. As shown in figure 4(b), the PCE values of both devices exhibited

a performance similar to that of OSCs fabricated on glass substrates. In OSCs with HNO₃-doped MLG electrodes, the PCE ranged between 2.5 and 2.6% during bending. A similar trend was also observed in OSCs with pristine MLG electrodes. In this case, the PCE ranged between 1.4 and 1.8% during bending. These results support the notion that chemically doped graphene electrodes can produce efficient and flexible OSCs on plastic substrates.

4. Conclusions

In conclusion, we have demonstrated flexible organic solar cells using chemically doped multilayer graphene films as transparent and conducting electrodes. The sheet resistance of the multilayer graphene films decreased by half after doping while maintaining similar transmittance, thereby enhancing the performance of the solar cells with doped graphene electrodes. Flexible organic solar cells with doped graphene electrodes on a plastic substrate retained a power conversion efficiency of 2.5–2.6%, regardless of the bending conditions, even up to a 5.2 mm bending radius.

Acknowledgments

The authors thank the National Research Laboratory Program, the National Core Research Center grant, and the World Class University program (R31-10026) of the Korean Ministry of Education, Science, and Technology.

References

- [1] Yu G, Gao J, Hummelen J C, Wudl F and Heeger A J 1995 *Science* **270** 1789
- [2] Brabec C J, Gowrisanker S, Halls J J M, Laird D, Jia S and Williams S P 2010 *Adv. Mater.* **22** 3839
- [3] Ji Y, Cho B, Song S, Kim T-W, Choe M, Kahng Y H and Lee T 2010 *Adv. Mater.* **22** 3071
- [4] Na S-I, Kim S-S, Jo J and Kim D-Y 2008 *Adv. Mater.* **20** 4061
- [5] Kumar A and Zhou C 2010 *ACS Nano* **4** 11
- [6] Lee B H, Park S H, Back H and Lee K 2011 *Adv. Funct. Mater.* **21** 487
- [7] Aguirre C M, Terson C, Paillet M, Desjardins P and Martel R 2009 *Nano Lett.* **9** 1457

- [8] Yeo J-S, Yun J-M, Kim S-S, Kim D-Y, Kim J and Na S-I 2011 *Semicond. Sci. Technol.* **26** 034010
- [9] Lee J-Y, Connor S T, Cui Y and Peumans P 2008 *Nano Lett.* **8** 689
- [10] Lee S et al 2011 *Appl. Phys. Lett.* **99** 083306
- [11] Geim A K and Novoselov K S 2007 *Nature Mater.* **6** 183
- [12] Ji Y, Lee S, Cho B, Song S and Lee T 2011 *ACS Nano* **5** 5995
- [13] Bae S et al 2010 *Nature Nanotechnol.* **5** 574
- [14] Matyba P, Yamaguchi H, Eda G, Chhowalla M, Edman L and Robinson N D 2010 *ACS Nano* **4** 637
- [15] Blake P et al 2008 *Nano Lett.* **8** 1704
- [16] De Arco L G, Zhang Y, Schlenker C W, Ryu K, Thompson M E and Zhou C 2010 *ACS Nano* **4** 2865
- [17] Choi Y-Y, Kang S J, Kim H-K, Choi W M and Na S-I 2012 *Sol. Energy Mater. Sol. Cells* **96** 281
- [18] Yin Z, Sun S, Salim T, Wu S, Huang X, He Q, Lam Y M and Zhang H 2010 *ACS Nano* **4** 5263
- [19] Dou L, You J, Yang J, Chen C-C, He Y, Murase S, Moriarty T, Emery K, Li G and Yang Y 2011 *Nature Photon.* **5** 480
- [20] Zhou H, Yang L, Stuart A C, Price S C, Liu S and You W 2011 *Angew. Chem. Int. Edn* **50** 2995
- [21] Kasry A, Kuroda M A, Martyna G J, Tulevski G S and Bol A A 2010 *ACS Nano* **4** 3839
- [22] Park H, Rowehl J A, Kim K K, Bulovic V and Kong J 2010 *Nanotechnology* **21** 505204
- [23] Lee S, Jo G, Kang S-J, Wang G, Choe M, Park W, Kim D-Y, Kahng Y H and Lee T 2011 *Adv. Mater.* **23** 100
- [24] Calizo I, Balandin A A, Bao W, Miao F and Lau C N 2007 *Nano Lett.* **7** 2645
- [25] Das A et al 2008 *Nature Nanotechnol.* **3** 210
- [26] Brabec C J, Dyakonov V and Scherf U 2008 *Organic Photovoltaics: Materials, Device Physics, and Manufacturing Technologies* (Weinheim: Wiley-VCH)
- [27] Irwin M D, Buchholz D B, Hains A W, Chang R P H and Marks T J 2008 *Proc. Natl Acad. Sci.* **105** 2783